

Oil-in-water microfluidics on the colloidal scale: new routes to self-assembly and glassy packings

Max Meissner and Jun Dong

H.H. Wills Physics Laboratory, University of Bristol, BS8 1TL, Bristol UK

Jens Eggers

Mathematics Department, University of Bristol, BS8 1TW, Bristol UK

Annala M. Seddon

*H.H. Wills Physics Laboratory, University of Bristol, BS8 1TL, Bristol UK and
Bristol Centre for Functional Nanomaterials, University of Bristol, BS8 1TL, Bristol UK*

C. Patrick Royall

*H.H. Wills Physics Laboratory, University of Bristol, BS8 1TL, Bristol UK
Chemistry Department, University of Bristol, BS8 1TS, Bristol UK
Department of Chemical Engineering, Kyoto University, Kyoto 615-8510, Japan and
Centre for Nanoscience and Quantum Information, Tyndall Avenue, Bristol, BS8 1FD, UK*

Microfluidic emulsification is a field primarily focused on water-in-oil with current work on the inverse oil-in-water systems concerning the production of droplets with sizes on the order of 10s of micrometres, large enough that Brownian motion is negligible. Here we introduce a new methodology to produce a colloidal model system of fluorescent labelled emulsion droplets suitable for particle resolved studies with confocal microscopy. To this end, we demonstrate a reliable method of generating a wide range of oil in water emulsions at the micron length scale. We have developed Norland Optical Adhesive (NOA) flow focusing devices, making use of the excellent solvent compatibility and surface properties of NOA, to generate droplets of a variety of oils with polydispersity as low as 3%. We analyse the structure of our emulsions in 3D with confocal microscopy and reveal a new monodisperse thermal system.

INTRODUCTION

The majority of work on colloidal systems concerns itself either with the study of solid particles, for example solid colloidal spheres, or with emulsions, where an oil phase is dispersed in an aqueous medium or vice versa[1]. For solid colloidal spheres, unsurprisingly, the ratio of particle viscosity to the suspending fluid viscosity, $\lambda = \eta_o/\eta_i$, will tend towards infinity. On the other hand emulsions are much "softer" with viscosity ratios λ much closer to 1. This allows emulsion droplets to function as exciting new colloidal model systems. For example, emulsion droplets have negligible friction at their surfaces with intriguing consequences for the jamming-glass transient crossover, alternatively, the ease of adsorption of lipids or polymers onto droplets opens new and exciting directions in self-assembly[2–6].

Emulsions, with their multitude of food, care product, and petrochemical applications [7, 8], are a system of great scientific and industrial interest, and so it should come as no surprise that the formation of emulsions is a well explored field with a huge range of emulsification techniques available. These methods include such techniques as mechanical milling, blending, high pressure homogenization, or shear mixing. While powerful, these techniques generally only produce large emulsion droplets, or emulsions with a broad size distribution. Microemulsions on the other hand, while extremely versa-

tile due to their self assembly behaviour, are generally in the range of 10-100nm, and thereby far too small for realspace imaging and coordinate tracking[9]. An emulsion that combines the best of both worlds possessing both an average droplet size in the range of a few microns, with a narrow size distribution, would open up a wide range of new possibilities.

An alternative to the aforementioned techniques is microchannel emulsification, a versatile technique where two or more distinct fluid phases are flowed through a microscale channel and interfacial stresses are induced to generate droplets with very narrow size distributions [10]. Currently microfluidic emulsification techniques remain focussed primarily on the formation of water-in-oil emulsions, usually with values of λ below 1.

In order to develop the desired colloidal model system we must first consider the behaviour of a droplet in solution using the Peclet number $Pe = \tau_B/\tau_{sed}$. Here this dimensionless parameter is the ratio between the time it takes for a particle to diffuse its own radius, $\tau_B = \sigma^3\pi\eta/8k_B T$, where σ is the particle diameter η is the solution viscosity and T is the temperature, and the time the particle takes to sediment by its diameter, $\tau_{sed} = \sigma/V_{sed}$, where V_{sed} is the sedimentation velocity $V_{sed} = \delta mg/3\pi\eta\sigma_H$, where δm is the bouyant mass and σ_H the hydrodynamic diameter. A Peclet number around one is generally seen as the dividing line between a colloidal system and an athermal granular system[11]. As the Peclet number scales with both

particle diameter and buoyant mass a colloidal emulsion can be achieved either by producing droplets of a sufficiently small diameter or by using liquids with suitably similar densities [12]. As such, it is vital that a microfluidic system for the production of colloidal oil-in-water emulsions is capable of both producing droplets which are suitably small and uniform, but also to be solvent-compatible enough to produce emulsions from a range of component materials.

Microfluidic droplet generation can generally be realised with three types of device: T-Junction devices where a slug of the dispersed phase is extruded into a flowing fluid until the dispersed phase fluid breaks up into droplets [13], co-flowing devices where an outer continuous phase fluid flows parallel to and surrounding an inner dispersed phase fluid until droplet generation occurs via stretching of the interface between the two fluids [14], and flow-focusing devices, where co-flowing streams are forced through a narrow aperture causing droplet breakup [15]. Here we consider flow-focusing devices, as these provide the best system for producing droplets with sizes smaller than those of the channel dimensions.

However, producing suitable oil-in-water emulsions via microfluidic methods remains challenging. The vast majority of microfluidic emulsification systems are manufactured using polydimethylsiloxane (PDMS). While PDMS is generally an excellent material for microfluidics [16] offering good solvent compatibility, good optical transmittivity, high flexibility and great durability, it is also strongly hydrophobic, preventing the formation of stable oil-in-water droplets [17]. Although techniques for making PDMS devices hydrophilic and thereby allowing stable droplet generation exist, these are either short lived such as plasma treatment [18] or involve sequential surface coatings [19] which are impractical for use with devices small enough to easily generate micron scale droplets.

Norland optical adhesives provide a viable alternative to PDMS for oil-in-water microfluidics [20, 21]. Their rapid curing speed, alongside their durability, makes them ideal for pattern transfer from PDMS molds. Additionally, while already natively more hydrophilic than PDMS, exposure to an Oxygen plasma forms a long-lasting hydrophilic surface, ideal for the formation of oil-in-water droplets [20]. Here we show a microfluidic flow focussing system based on the use of NOA microfluidics for the generation of monodisperse oil in water emulsions which can produce droplets on the micron scale with polydispersities of below 5%. To demonstrate the utility of this technique, we use the topological cluster classification to investigate the higher order structure of an filled capillary of emulsion droplets, and compare this to a simulated hard sphere system.

This paper is organised as follows. In the materials and methods section first we describe the micro-fabrication and polymer casting process of the Norland flow-focusing devices used. In the same section we briefly describe the flow focusing process used to generate micron scale

emulsions and the confocal microscopy and coordinate tracking techniques. The topological cluster classification algorithm is used to analyse the structure of the resulting packings. In the results section we describe the droplet sizes produced and demonstrate the excellent size selectivity of this method for varying flow rate and the droplet formation behaviour for various viscosity ratios. We then describe the structural insights obtained from using the topological cluster classification algorithm for probing the structure of an emulsion is discussed, and our emulsion is compared to a simulated hard sphere system. Finally, we briefly summarise our work and the scientific implications thereof in the conclusions section.

MATERIALS AND METHODS

Imaging

Droplet formation in the microfluidic channels was imaged using a Leica DMI 3000B Brightfield microscope. High speed droplet production was imaged using exposure times of $250\mu s$. Confocal microscopy as per established methods [11, 22, 23] was employed to obtain 3-dimensional images of an emulsion filled glass capillary. The imaged region consisted of region containing $N \approx 3 \cdot 10^3$ polydimethylsiloxane (PDMS) droplets within an area of cross section $128.8\mu m$ by $128.8\mu m$ with a vertical height of $60.1\mu m$. The entire region was imaged with a LEICA SP8 confocal microscope with an excitation wavelength of $485nm$.

Microfluidic Fabrication

Device patterns shown in Fig.1 were etched on to silicon wafers using standard photolithographic methods. Etched wafers were treated with Trichloro(1H,1H,2H,2H-perfluorooctyl) silane to allow easy polymer lift-off. Sylgard 184 Silicone elastomer was poured on the silicon wafers, degassed under vacuum, and heat cured at $60^\circ C$ for 6 hours. PDMS layers were cut from the silicon wafer, thoroughly cleaned with deionised water and ethanol. Norland optical adhesive (NOA) 81 was poured onto the prepared PDMS pattern and cured under $365nm$ UV radiation for 30 minutes. Tubing connectors were drilled into the NOA chips using a drill, and the drilled chips were cleaned with ethanol and deionised water. NOA channels were made hydrophilic by exposing the device layer to a $100w$ Oxygen plasma for 60 seconds.

The channel geometry was enclosed by sealing the NOA chip with a thin layer of NOA produced by sandwiching several droplets of NOA between two clean sheets of PDMS and UV curing for 2 minutes.

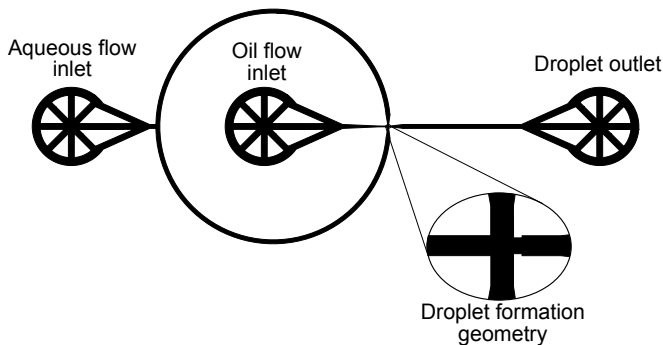


FIG. 1. Schematic of device layout. Popout image shows droplet formation geometry, channels measure $50\mu\text{m}$ before narrowing down to a $8\mu\text{m}$ aperture, inducing shear stress and leading to droplet formation.

Droplet formation

Flow rate tests were carried out by connecting the assembled NOA chip to a nitrogen driven pressure pump (Fluigent MFCS) with polyethylene tubing. 16mMol sodium dodecyl sulphate(SDS) aqueous solution was used as the continuous phase, and pressure and flow rate were controlled using MaesFlo 3.2 software (Fluigent, Paris, France). Flow rates were adjusted until the oil flow was stable and producing droplets. Once stable droplet formation was achieved, flow rate ratios were adjusted throughout the experimental range. Viscosity ratio measurements were carried out by varying both the oil phase used, as well as the viscosity of the aqueous phase. The liquid combinations used were an 80/20 cis-decalin/Bromo-cyclohexane mix with 16mMol sds in deionised water, an 80/20 cis-decalin/chb mix with 16mMol SDS in a 1:1 mix of deionised water and glycerol, and dodecane with 16mMol SDS deionised water.

Droplets were subsequently collected by allowing stable droplet collection to proceed long enough to drive the produced emulsion into a 1ml Eppendorf vial, transferred into a glass capillary and imaged on a leica brightfield microscope. Droplet sizing was carried out as shown in Fig.3(a) where the size was taken directly from the image.

For the purpose of analysis using the topological cluster classification (TCC) analysis, droplets were produced as above using a system of 5cP Polydimethylsiloxane oil dyed with Nile red as the internal fluid and 32mMol sodium dodecyl sulfate solution as the outer fluid. Produced droplets were then collected and diluted with 50% by weight glycerol in order to match refractive indices between the aqueous and non-aqueous phases. The index matched emulsion was filled into a capillary and imaged using confocal laser scanning microscopy on a Leica confocal microscope. A $512 \times 512 \times 256$ pixel image was taken and coordinate tracking was carried out using the Colloids particle tracking package[24], this tracking method identifies particle centres by searching for a Gaussian of the image intensity and produces XYZ coordinates for

each detected particle. XYZ coordinates of particle centers were used to calculate a 3D $g(r)$ and the Topological Cluster Classification (TCC) was used to interpret cluster populations[25].

Topological cluster classification

The Topological cluster classification (TCC) algorithm works by searching for a configuration of particles with a bond network similar to that found in a corresponding minimum free energy cluster of up to 15 particles in a bulk assembly of spheres[25]. By identifying clusters related to specific interaction potentials, the TCC provides a direct link between the interactions in the system and any structural ordering found. The algorithm functions as follows: first the neighbors of each particle are identified, then the network of particles and neighbors is searched for rings of 3, 4, and 5 particles. From these rings a set of "basic-clusters" is identified, and distinguished by the number of particles that are common neighbors. Larger clusters are then identified by combining these basic clusters yielding structures with bond networks similar to the minimum energy clusters as pictured in Fig.6(c)[26]. The topological cluster classification data obtained in this way is compared against molecular dynamics simulations carried out in Dynamo[27] using previously established simulation parameters[28].

RESULTS AND DISCUSSION

Droplet production was observed and investigated under a range of flow conditions, and a strong size scaling between droplet size and flow rate ratio was observed. This relationship held true for several different solvent systems of varying viscosity ratio λ . Droplet radius and flow rate ratio were compared and two separate droplet production modes, the geometry controlled and the dripping modes, were observed. By tuning the relative flow rates droplets of a desired size and quality were then collected. To demonstrate the utility of our emulsion system as a colloidal model system, coordinate tracking and topological cluster classification analysis was carried out on the emulsion sample. This analysis showed a large fraction of the emulsion droplets were oriented as 10 membered defective icosahedra suggesting that the emulsion has a structure comparable to a supercooled liquid.

Droplet production

Droplet formation proceeded in a stable manner between Q_o/Q_i values of 1 to 60, outside of this range droplet formation is inhibited either by dewetting of the outer phase, or by channel filling of the inner phase.

TABLE I. Liquid phases used to produce the emulsion systems considered

| Oil phase | Aqueous Phase | η_o/η_i |
|------------------------------------|--------------------------------|-----------------|
| 80:20 Cis-decalin/Bromocyclohexane | Deionised water | 0.3 |
| 80:20 Cis-decalin/Bromocyclohexane | 50:50 Deionised water/Glycerol | 1.5 |
| Dodecane | 50:50 DIW/Glycerol | 3.8 |

Within this range of Q_o/Q_i the formation of droplets was observed via two distinct mechanisms. Droplet formation in a microfluidic device is governed by three main parameters, the ratio of flow rate of the outer fluid to the inner fluid Q_o/Q_i , the ratio of the outer and inner fluid viscosities $\lambda = \eta_o/\eta_i$, and the capillary number $Ca = \eta_o G a_o / \gamma$ where G is a characteristic deformation rate and a_o is the characteristic droplet radius. Of particular importance here is the capillary number, a parameter influenced by the geometry of the device as well as the flow rate of the fluid being considered[29]. Depending on the capillary number and thereby the flow rate ratio Q_o/Q_i , it is possible to select between two separate modes of droplet production. At lower capillary numbers, of order 10^{-2} , geometry controlled droplet formation occurs as shown in Fig.2(a). In this mode the fluid interface stretches through the aperture and obstructs, leading to a pressure spike followed by droplet breakup. For this mode a weak scaling with flow rate is expected and droplet size is roughly the same as the channel geometry[30]. At higher values of the flow rate ratio Q_o/Q_i , with capillary number of order 10^{-1} this geometry controlled mode gives way to the dripping mode of droplet formation as shown in Fig.2(b). The fluid interface in a dripping microfluidic device narrows into a fluid tendril, with the droplet drop off remaining stationary and within the constriction. This mode of formation yields droplets smaller than the device geometry[31].

Once a stable formation regime was established, an emulsion produced at a fixed Q_o/Q_i value of 40 was collected on the millilitre scale. Droplets produced in this way are shown in Fig.3(a) and were found to have radii of $3.3 \mu\text{m}$ with a polydispersity, here defined as the relative standard deviation, of 4.8

Varying the viscosity ratio of the outer to inner phase, η_o/η_i , lead to some striking differences in droplet produc-

tion. At a low value η_o/η_i of 0.3, droplet production was stable throughout the largest range of flow rates, with droplet size scaling inversely with flow rate as shown in Fig.4a. At value of η_o/η_i of 1.5, stable droplet formation was found to occur in a much narrow band of Q_o/Q_i , in particular droplet formation also seemed to be produced in two general methods depending on the total net flow rate as shown in Fig.4(b) this striking difference between two methods of flow seems to suggest a switch between two different modes of droplet behaviour. Finally, at a value of η_o/η_i of 3.8, droplet formation was highly unstable, and droplets produced were generally twice as large as at lower flow rates, with average radii above $6 \mu\text{m}$. Surprisingly we find that droplet formation proceeds in a more stable manner at lower values of Q_o/Q_i , with only a small trade off in droplet size.

As shown in Fig.4 and 5 our microfluidic system demonstrates a high degree of versatility in the size of droplets produced. By varying Q_o/Q_i , a wide range of droplet sizes was produced with excellent size selectivity. Droplets produced ranged in radius from $2 \mu\text{m}$ to $12 \mu\text{m}$ and droplet size was observed to be in good agreement with predictions by Garstecki et. al[30] as shown by the linear scaling of the log-log plot of droplet diameter, σ and the flow rate ratio Q_o/Q_i in Fig.5 suggesting a dripping mode of droplet production.

Emulsion structure

In a dense assembly of spheres tetrahedra and consequently five membered clusters consisting of two tetrahedra are rapidly formed, with particles arranged as members of these locally favoured structures having lower potential energies and slower dynamics[32]. Organisation of these tetrahedra into larger clusters can be suppressed

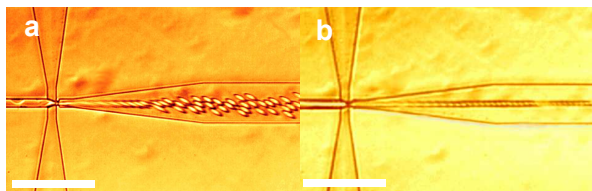


FIG. 2. (a) Image of geometry controlled droplet production with droplets roughly 40% larger than channel dimensions (b) image of of droplet production via a different mode of droplet production where droplet snap-off occurs within the confines of the geometry producing droplets roughly 10% smaller than channel dimensions. Scale bars represent $100 \mu\text{m}$

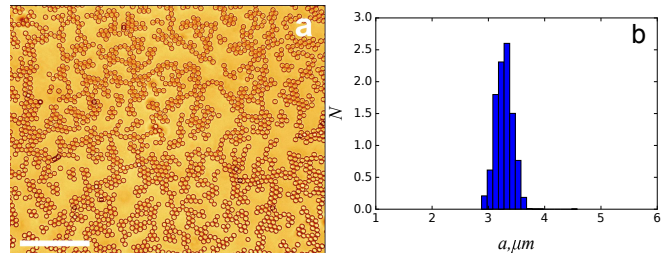


FIG. 3. (a) Dodecane droplets with mean radius, a of $3.3 \mu\text{m}$ and polydispersity of 4.8% produced in a Noa 81 microfluidic device. Scale bar represents $100 \mu\text{m}$ (b) Normalized histogram of droplet size distribution.

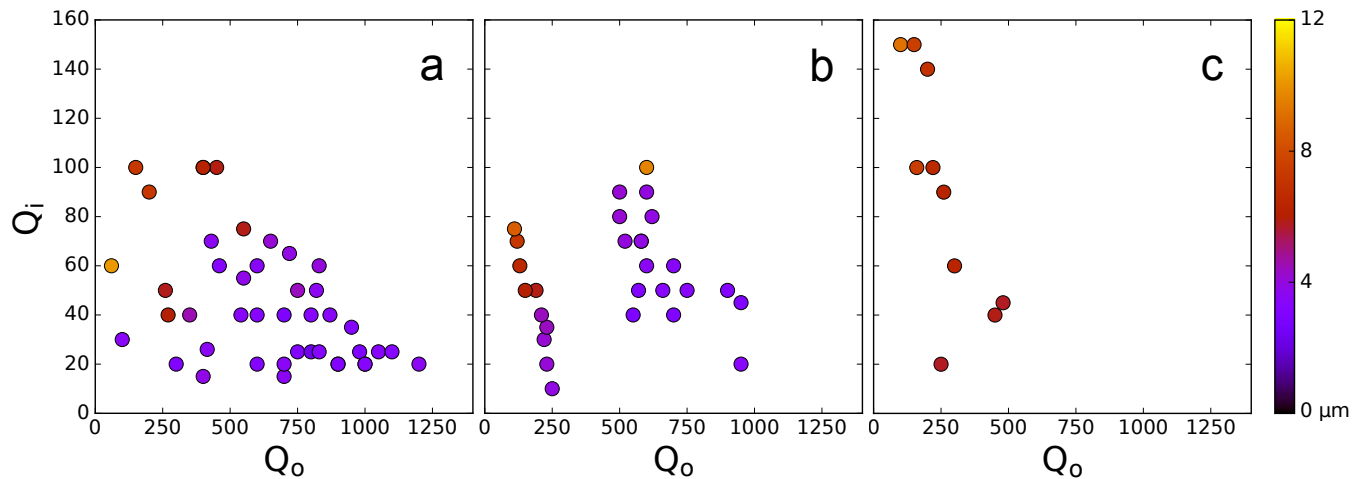


FIG. 4. Heatmaps of droplet radius against continuous and discrete phase flow rates for 3 different values of the viscosity ratio λ , (a) 0.3, (b) 1.5, and (c) 3.8. Flow rates Q_o , and Q_i are shown here in units of nl/min

due to dynamical arrest with the system unable to reach an equilibrated configuration for which the formation of larger clusters is expected. Due to this gels and glasses, as well as athermal systems would be dominated by tetrahedra, while systems which are thermal, and in which reorganisation can occur would be dominated by higher membered clusters [33] [34]. In an emulsion system which is thermal we would expect to see significantly more $m=12$ and $m=11$ structures, where m is the number of particles in the structure, than $m=5$ structures. This is exactly what we see in our TCC analysis shown in Fig.6(c) where a significantly larger proportion of higher membered clusters suggest that our system is a thermal sys-

tem analogous to a supercooled liquid [25]. Interestingly compared to a hard sphere system of comparable volume fraction, ($\phi = 0.4$), as shown in yellow in Fig.6(c) our emulsion system contains a much higher portion of $m=12$ and $m=11$ clusters as well, suggesting significantly easier rearrangement into higher order structures, likely due to the ease of deformation of emulsion droplets. Finally, we note that the emulsion studied here contains a much larger number of the structures analysed, we propose that this arises due to a charge effect facilitating easier cluster formation.

CONCLUSIONS

In this work we have demonstrated a powerful and versatile microfluidic droplet generator for the production of oil-in-water emulsions, and shown that this system produces droplets of a wide range of sizes with extremely low polydispersity. By utilising the favourable mechanical and surface chemical properties of Norland optical adhesives we open up a new and promising parameter space for studying colloidal systems with carefully tuned chemistry and viscosity ratios. We demonstrate the potential of this system as a colloidal model system by studying the arrangement of emulsion droplets with respect to locally favoured structures and as shown in Fig.6(c) are able to obtain detailed information as to the local structure of a highly uniform emulsion. By comparing the population of $m=10$ defective icosahedral clusters compared to the intermediate $m=5$ bi-tetrahedron cluster we observe that as expected of a deformable and surface smooth particle system, the silicone oil emulsion is not arrested and capable of rearrangement, behaving much like a supercooled fluid. We believe that this microfluidic system shows great potential as a powerful tool for studying exciting new colloidal behaviour, and in particular by carefully

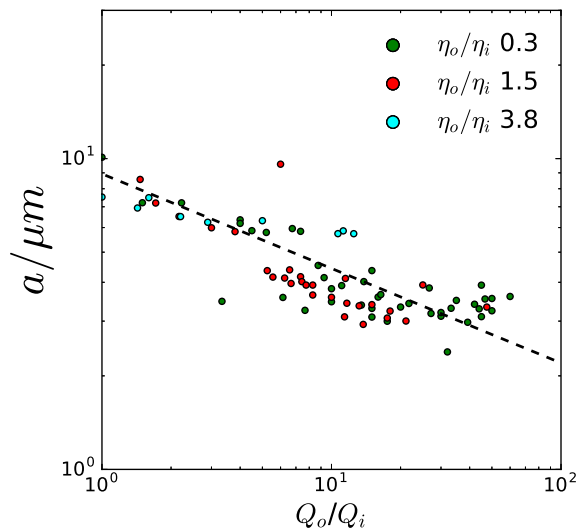


FIG. 5. Log-Log plot with a line to guide the eye showing strong scaling of droplet size with flow rate ratio, in particular this scaling behaves similarly regardless of the viscosity ratio of the two fluids.

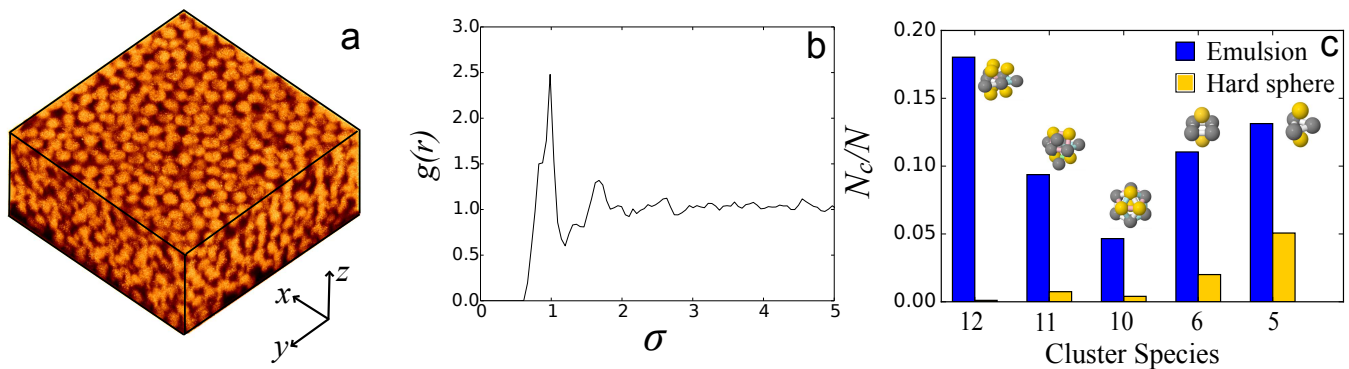


FIG. 6. Image showing (a) Representation of 3 dimensional confocal image of silicone oil emulsion with dimensions of $128.8 \times 128.8 \times 60.1 \mu m$, (b) radial distribution function of emulsion droplets and (c) Topological cluster classification chart, showing relative population of locally favoured icosahedral cluster species for our emulsion in blue, and a hard sphere system of comparable volume fraction ($\phi = 0.4$) in yellow.

turning the microfluidic flow properties and the relative fluid densities the technique demonstrated here can allow the production of truly colloidal emulsions with tunable size, size distribution, and composition.

ACKNOWLEDGEMENTS

The authors would like to thank Oliver Dauchot and Francesco Turci for many helpful discussions. M.M. acknowledges the EPSRC Doctoral training allowance, CPR acknowledges the Royal Society and Kyoto University SPIRITS fund for financial support, JD and CPR acknowledge the European Research Council (ERC consolidator grant NANOPRS, project number 617266), and JD acknowledges Bayer CropScience AG for financial support.

-
- [1] Robert J. Hunter. *Foundations of colloid science*. Oxford University Press, 2001.
- [2] T. G. Mason and D. A. Weitz. Optical measurements of frequency-dependent linear viscoelastic moduli of complex fluids. *Physical Review Letters*, 74(7):1250–1253, 1995.
- [3] Lang Feng, Lea-Laetitia Pontani, Rémi Dreyfus, Paul Chaikin, and Jasna Brujic. Specificity, flexibility and valence of DNA bonds guide emulsion architecture. *Soft Matter*, 9(41):9816, 2013.
- [4] Stef a J Van Der Meulen and Mirjam E. Leunissen. Solid colloids with surface-mobile DNA linkers. *Journal of the American Chemical Society*, 135(40):15129–15134, 2013.
- [5] Kenneth W. Desmond, Pearl J. Young, Dandan Chen, and Eric R. Weeks. Experimental study of forces between quasi-two-dimensional emulsion droplets near jamming. *Soft Matter*, 9(12):3424–3436, 2013.
- [6] Chi Zhang, Cathal B. O’Donovan, Eric I. Corwin, Frdric Cardinaux, Thomas G. Mason, Matthias E. Mbius, and Frank Scheffold. Structure of marginally jammed polydisperse packings of frictionless spheres. *Physical Review E - Statistical, Nonlinear, and Soft Matter Physics*, 91(3):1–6, 2015.
- [7] Christianto Wibowo and Ka M. Ng. Product-oriented process synthesis and development: Creams and pastes. *AIChE Journal*, 47(12):2746–2767, 2001.
- [8] Job Ubbink. Soft matter approaches to structured foods: from cook-and-look to rational food design? *Faraday Discussions*, 158:9, 2012.
- [9] Julian Eastoe, Marios Hopkins Hatzopoulos, and Rico Tabor. Microemulsions. In *Encyclopedia of Colloid and Interface Science*, pages 688–729. Springer Berlin Heidelberg, 2013.
- [10] H.A Stone and S Kim. Microfluidics: basic issues, applications, and challenges. *AIChE Journal*, 47(6):1250–1254, 2001.
- [11] Alexei. Ivlev, Hartmut Löwen, Gregor Morfill, and C. Patrick Royall. *Complex plasmas and colloidal dispersions : particle-resolved studies of classical liquids and solids*. World Scientific, 2012.
- [12] Adam Wysocki, C. Patrick Royall, Roland G Winkler, Gerhard Gompper, Hajime Tanaka, Alfons Van Blaaderen, and Hartmut Löwen. Direct observation of hydrodynamic instabilities in driven non-uniform colloidal dispersions. *Soft Matter*, 5(7):4, 2008.
- [13] Todd Thorsen, Richard W. Roberts, Frances H. Arnold, and Stephen R. Quake. Dynamic pattern formation in a vesicle-generating microfluidic device. *Physical Review Letters*, 86(18):4163–4166, 2001.
- [14] a M Gañán-Calvo and J M Gordillo. Perfectly monodisperse microbubbling by capillary flow focusing. *Physical review letters*, 87(27 Pt 1):274501, 2001.

- [15] Shelley L. Anna, Nathalie Bontoux, and Howard a. Stone. Formation of dispersions using "flow focusing" in microchannels. *Applied Physics Letters*, 82(3):364–366, 2003.
- [16] J Cooper McDonald and George M Whitesides. Poly (dimethylsiloxane) as a Material for Fabricating Microfluidic Devices. *Accounts of Chemical Research*, 35(7):491–499, 2002.
- [17] Honest Makamba, Jin Ho Kim, Kwansoep Lim, Nokyoung Park, and Jong Hoon Hahn. Surface modification of poly(dimethylsiloxane) microchannels. *Electrophoresis*, 24(21):3607–3619, 2003.
- [18] Dhananjay Bodas and Chantal Khan-Malek. Hydrophilization and hydrophobic recovery of PDMS by oxygen plasma and chemical treatment. An SEM investigation. *Sensors and Actuators B: Chemical*, 123(1):368–373, 2007.
- [19] Wolfgang-Andreas C. Bauer, Martin Fischlechner, Chris Abell, and Wilhelm T. S. Huck. Hydrophilic PDMS microchannels for high-throughput formation of oil-in-water microdroplets and water-in-oil-in-water double emulsions. *Lab on a Chip*, 10(14):1814, 2010.
- [20] Ph. Wägli, A. Homsy, and N.F. de Rooij. Norland optical adhesive (NOA81) microchannels with adjustable wetting behavior and high chemical resistance against a range of mid-infrared-transparent organic solvents. *Sensors and Actuators B: Chemical*, 156(2):994–1001, 2011.
- [21] S.H. Kim, Y. Yang, M. Kim, S.-W. Nam, K.-M. Lee, N.Y. Lee, Y.S. Kim, and S. Park. Simple Route to Hydrophilic Microfluidic Chip Fabrication Using an Ultraviolet (UV)-Cured Polymer. *Advanced Functional Materials*, 17(17):3493–3498, 2007.
- [22] Alfons van Blaaderen and Pierre Wiltzius. Real-space structure of colloidal Hard-Sphere Glasses. *Science*, 270(19):1177, 1995.
- [23] U. Gasser, Eric R. Weeks, Andrew Schofield, P N Pusey, and D A Weitz. Real-Space Imaging of Nucleation and Growth in Colloidal Crystallization Published by : American Association for the Advancement of Science Linked references are available on JSTOR for this article : Real-Space Imaging of Nucleation and Growth in. *Science*, 292(5515):258–262, 2001.
- [24] Mathieu Leocmach and Hajime Tanaka. A novel particle tracking method with individual particle size measurement and its application to ordering in glassy hard sphere colloids. *Soft Matter*, 9(5):1447–1457, 2013.
- [25] C. Patrick Royall, Stephen R. Williams, and Hajime Tanaka. The nature of the glass and gel transitions in sticky spheres. *Cond-Mat.Soft*, (SEPTEMBER 2014):12, 2014.
- [26] Alex Malins, Stephen R. Williams, Jens Eggers, and C. Patrick Royall. Identification of structure in condensed matter with the topological cluster classification. *Journal of Chemical Physics*, 139(23), 2013.
- [27] M. N. Bannerman, R. Sargant, and L. Lue. DynamO: a free O(N) general event-driven molecular dynamics simulator. *Journal of computational chemistry*, 32(15):3329–38, 2011.
- [28] C. Patrick Royall, Alex Malins, Andrew J. Dunleavy, and Rhiannon Pinney. Strong geometric frustration in model glassformers. *Journal of Non-Crystalline Solids*, 407:34–43, 2015.
- [29] Shelley L. Anna. Droplets and Bubbles in Microfluidic Devices. *Annual Review of Fluid Mechanics*, 48(1):annurev-fluid-122414-034425, 2016.
- [30] Piotr Garstecki, Howard A. Stone, and George M. Whitesides. Mechanism for Flow-Rate Controlled Breakup in Confined Geometries: A Route to Monodisperse Emulsions. *Physical Review Letters*, 94(16):164501, 2005.
- [31] Shelley L. Anna and Hans C. Mayer. Microscale tip-streaming in a microfluidic flow focusing device. *Physics of Fluids*, 18(12):121512, 2006.
- [32] S. Mazoyer, F. Ebert, G. Maret, and P. Keim. Correlation between dynamical heterogeneities, structure and potential-energy distribution in a 2D amorphous solid. *European Physical Journal E*, 34(9):101, 2011.
- [33] C. Patrick Royall, Stephen R Williams, Takehiro Ohtsuka, and Hajime Tanaka. Direct observation of a local structural mechanism for dynamic arrest. *Nature materials*, 7(July):556–561, 2008.
- [34] Jade Taffs, Stephen R. Williams, Hajime Tanaka, and C. Patrick Royall. Structure and kinetics in the freezing of nearly hard spheres. *Soft Matter*, 9:297–305, 2013.